JCTC Journal of Chemical Theory and Computation

Article

pubs.acs.org/JCTC

Local Hybrid QM/QM Calculations of Reaction Pathways in Metallobiosites

Milica Andrejić and Ricardo A. Mata*

Institut für Physikalische Chemie, Georg-August-Universität Göttingen, Tammannstrasse 6, D-37077 Göttingen, Germany

Supporting Information

ABSTRACT: The accurate calculation of activation barriers is fundamental for the modeling of reaction pathways. However, the computational cost of describing electronic correlation at metal sites can be a deterrent. A possible solution to this problem is the use of hybrid QM/QM approaches, which combine different levels of theory in a single calculation. In this way, the metal and its direct vicinity can be treated, for example, with a coupled cluster method, with the remaining system at the MP2 level. We present calculations on two selected molybdenum complexes modeling the active sites of sulfite oxidase and dimethyl sulfoxide reductase. Use is made of the LMOMO scheme, a hybrid QM/QM model that enables the partition of the system directly at the orbital level, thus avoiding the use of model systems. The results show that even when the high-level calculations are restricted to the orbitals directly located at the metal atom, most of the electronic correlation effects are captured.

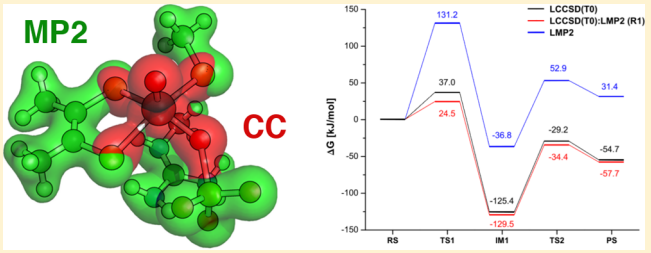

1. INTRODUCTION

Metal-mediated catalysis is ubiquitous in nature. It is estimated that about one-third of all enzymes contain at least one metal atom in the active site. However, the description of such metallobiosites by quantum-chemical methods presents a considerable challenge.[1] Namely, in the case of transition metals, the accurate treatment of electronic correlation effects is mandatory. This may include both static and dynamic effects. The importance of static correlation depends on the electronic configuration of the metal and possible state degeneracies. Dynamic correlation, however, is always a factor, given that such reactions proceed through changes in the coordination of the complex and are oftentimes of redox nature. Therefore, higher-order excitations should be included and/or multi-reference approaches applied. Adding to the problem, it is oftentimes difficult to describe such active sites with simplified model systems. The ligands directly coordinated to the metal sites are usually too large to address with correlated wave function methods. The use of coupled cluster (CC) approaches, for example, is often limited to the smallest possible model systems, with ligands not much larger than ammonia or water. These are almost exclusively used for benchmark purposes.[2]

The use of hybrid QM/QM approaches opens up a range of new possibilities to deal with such systems. Given that electronic structure changes in the course of a reaction are oftentimes local, one can address them by targeting specific atom regions. The ONIOM method[3] is perhaps the most popular variant in the field. In this approach, separate runs are carried out in model structures of the active site, thereby providing a correction to a low-level calculation on the full system. However, this requires an adequate partitioning. The electronic structure of the model should not differ significantly from the full calculation. This can sometimes be difficult when dealing with transition-metal complexes. Subtle changes in the ligands can have a strong effect on the electronic states.

An alternative to the use of model systems has been suggested for carrying out QM/QM calculations. The LMOMO method makes use of the pair approximations in local correlation methods to apply different levels of theory in selected regions.[4] The method has been applied to a series of reactions, showing that it is possible to combine CC and second-order Møller–Plesset perturbation theory (MP2) in a single calculation and systematically approach the high-level reference values. Comparisons have also been made to ONIOM. The main advantage is to avoid breaking and saturating covalent bonds, which allows for a wider application range. Our method is based on the Pulay–Saebø formulation,[5,6] whereby the occupied space is described through localized molecular orbitals (LMOs) and the virtual space through nonorthogonal projected atomic orbitals (PAOs). However, the same rationale can be followed using other orbital spaces. Several different approaches to local correlation methods have been proposed over the years, and in most cases the extension would be straightforward.[7,8] Hybrid QM/QM methods similar to LMOMO have already been developed under the cluster-in-molecule approach.[9,10]

In this study, we tested the application of the LMOMO method to reactivity in bioinorganic complexes. The results,

Received: September 12, 2014

   dx.doi.org/10.1021/ct5008313 | J. Chem. Theory Comput. XXXX, XXX, XXX–XXX

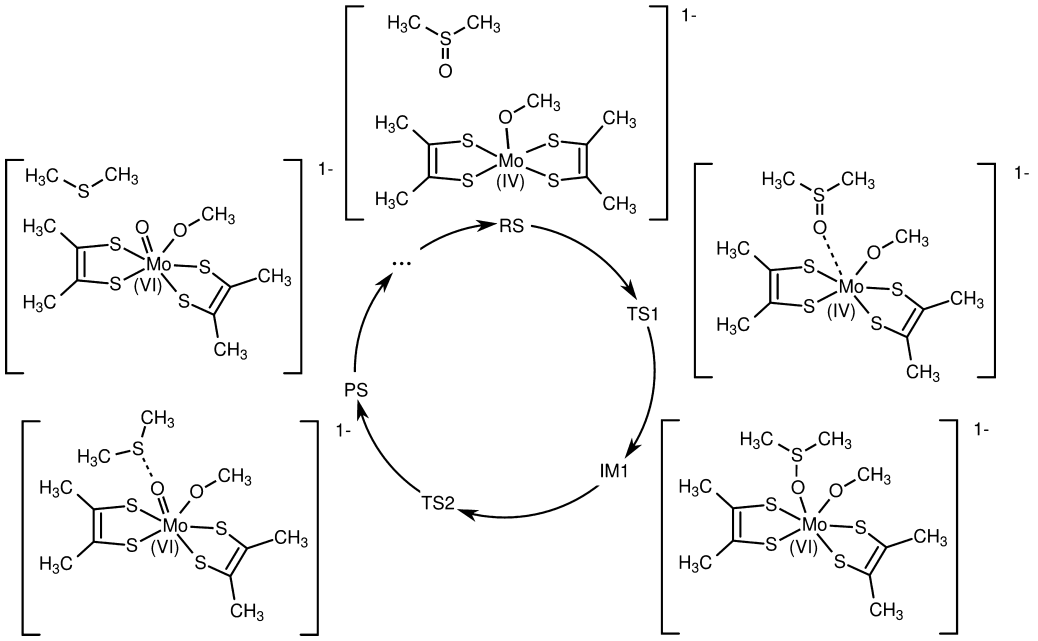

Figure 1. Reaction scheme for the reduction of dimethyl sulfoxide to dimethyl sulfide catalyzed by DMSOR. The scheme is shown for the cluster used in this study to model the active site. The molybdopterin ligand has been replaced by DMDT and a serine residue by methoxide.

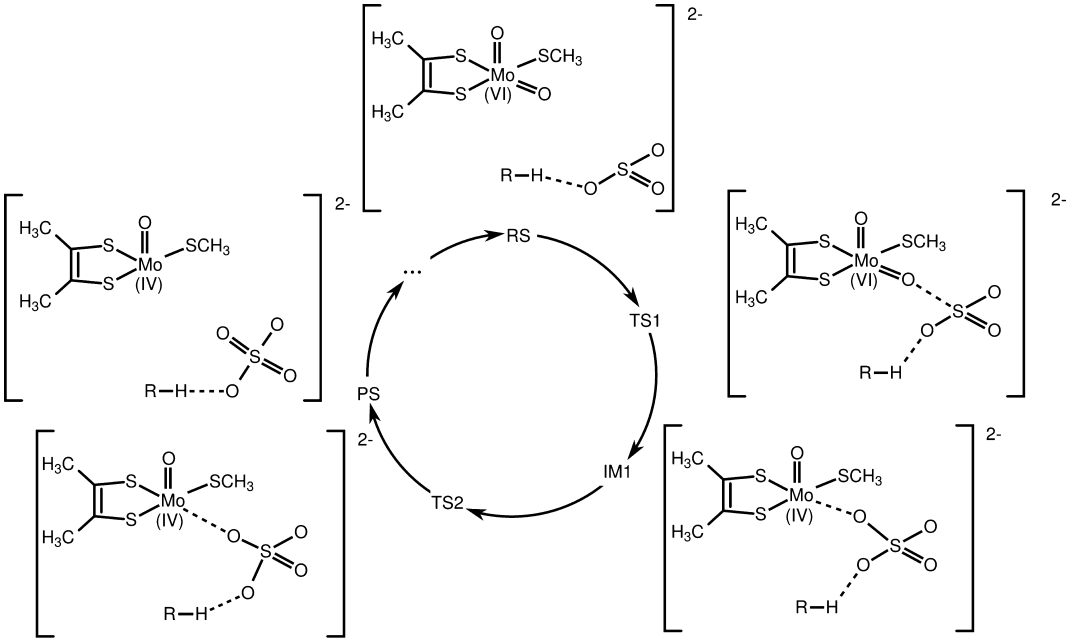

Figure 2. Reaction scheme for the oxidation of sulfite in SO following S→O mechanism. The scheme is shown for the cluster used in this study to model the active site. The molybdopterin ligand has been replaced by DMDT and a cysteine residue by methyl thiolate.

however, should also provide insight on how other local-correlation-based hybrid methods should perform. We considered rate-determining steps in the catalytic cycle from two of the main Mo enzyme families.[11] One set of calculations dealt with the dimethyl sulfoxide reductase (DMSOR) system. This enzyme catalyzes oxygen atom transfer from dimethyl sulfoxide (DMSO) to the Mo^{IV} metal center. This results in oxidation of the site to Mo^{VI} and the formation of dimethyl sulfide (DMS). The reaction scheme, which has been the target of numerous theoretical studies,[12−22] is depicted in Figure 1.

The second system we considered is the enzyme sulfite oxidase (SO), which catalyzes the conversion of SO_3^{2-} to SO_4^{2-}. There is an ongoing debate on the mechanism followed in this particular case. In the theoretical study carried out by Hernandez-Marin and Ziegler,[23] the reaction pathway depicted in Figure 2 was optimized and found to be in relatively good agreement with the experimentally derived reaction barrier. In this mechanism, the reaction starts with the formation of a bond between the sulfur atom and the equatorial oxygen. Other mechanisms have been put forward,[24,25] including intermediate coordination of the sulfur to the metal. In a recent study involving the present authors, three different reaction pathways were compared, and it was found that direct S→O coordination is the most favorable one.[26] However, the reaction energies

dx.doi.org/10.1021/ct5008313 | J. Chem. Theory Comput. XXXX, XXX, XXX−XXX

computed in the latter study were found to be excessively high. In the case of ref 23, the model system included an arginine residue interacting with the charged substrate. This strongly stabilized the transition-state energies. A more balanced description of the reaction would require an explicit description of the active site, possibly through a QM/MM study, as it includes several charged/polar residues that can strongly influence the energetics. However, since such studies are still underway, we opted to make use of structures including a single methylguanidinium group to model this particular arginine, since the latter has been found to be essential for the enzyme function.[27]

The two featured systems were chosen because of their similarities but also some specific properties. First of all, both deal with oxygen atom transfer reactions. The main difference is that they proceed in different directions (to and from the metal). Second, the reactive species are found to be most stable in the singlet state, allowing us to make exclusive use of closed-shell methods. Another issue is the multireference character of the intermediates under study. Our observations seem to indicate that small multireference effects are present. These are significant enough for the MP2 results to be nonsensical but still low enough for single-reference CC methods to be applicable. In the following section, we present a brief review of the LMOMO method, together with a description of the regions used in our calculations.

2. METHOD

The LMOMO approach builds upon the family of local correlation methods first introduced by Pulay[5,6] and later developed by Werner, Schütz, and co-workers.[28−30] After the Hartree−Fock calculation, the occupied orbitals are localized and projected out of the atomic orbital (AO) space to generate PAOs. The latter are used as a virtual space and are inherently local by construction. They are indexed to the same atomic centers as the original AOs and are grouped together in orbital domains specific to each occupied orbital ($[i]$). The domains for pairs and triples are constructed by union of the orbital domains ($[ij] = [i] \cup [j]$). The definition of the orbital domains depends on the criterion chosen to assign atomic centers to each occupied orbital. The Boughton−Pulay criterion has been commonly used for the past years.[31] It is based on the Löwdin atomic partial charges of the occupied orbitals and also overlap criteria. We have found that more consistent results can be obtained with resource to natural population analysis.[32,33] In this case, one calculates the charge of a given occupied orbital i at each atomic site. This is given by

$$P_{A,i} = \sum_{r\in\{A\}} \left(\frac{V_{ri}^{\,2}}{\sum_j V_{rj}^{\,2}} \right) \tilde{D}_{rr} \qquad (1)$$

where the matrix $\mathbf{V}$ is the transformation matrix from natural atomic orbitals (NAOs) to the local occupied orbitals and $\tilde{D}_{rr}$ is the occupation number for a given NAO r. The sum runs over the PAOs located at atom A. If the charge exceeds a defined threshold (T_{NPA}), the occupied orbital domain will include the atom PAOs. We have found that a threshold of $0.03e$ gives rather consistent results in a large variety of molecular systems.[33−38]

All of the steps mentioned so far are performed in any regular LMP2 or local CC calculation. The difference in LMOMO is that the occupied orbitals and their respective domains are split into groups and different methods are applied to each group. Since it would be impractical to select individual orbitals, a list of atoms is instead used. The orbital domains define where each orbital is located. More details on the region selection can be found in the original paper.[4] We make use of the same "high level:low level" nomenclature applied in other QM/QM schemes, meaning that a combination of LCCSD with LMP2 is denoted as LCCSD:LMP2. Three different regions are supported in the current program version. In the case of LCCSD:LMP2 or LCCSD(T0):LMP2 calculations, the CC amplitudes can be coupled to the MP2 amplitudes of another region by including them as fixed values in the CC residuals. We applied this in all of our calculations for all pairs within 5 bohr of the high-level region.

Taking advantage of the similarities between the two systems, we considered three main selections for the LMOMO calculations. We followed a similar reasoning for both pathways. The high-level regions are represented in red in Figure 3, taking

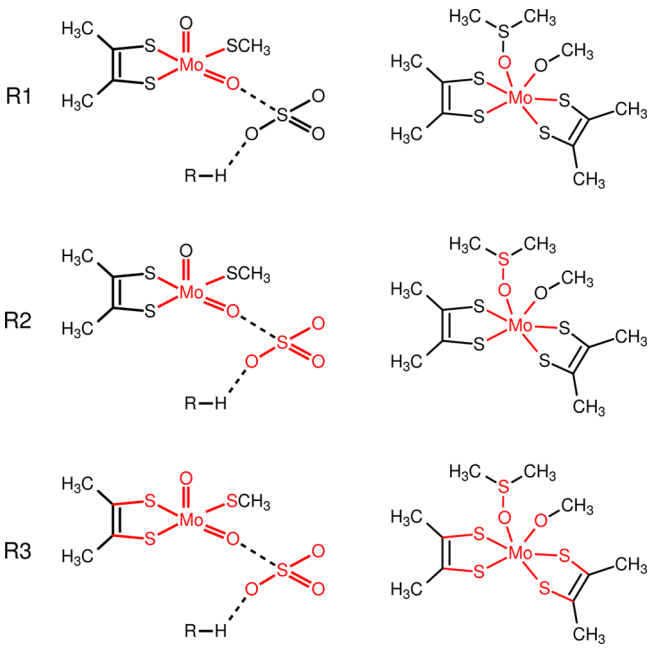

Figure 3. High-level region selections for the SO reaction (left side) and DMSOR (right side). The number of orbitals included in the high-level regions were 15/17 (R1), 27/20 (R2), and 33/28 (R3) from a total of 61/57 valence orbitals for SO/DMSOR.

the TS2 structure for the SO system and IM1 for DMSOR as examples. In a first set, we included only orbitals with the metal site in their domain list. In other words, if the partial charge of an orbital at the Mo atom exceeded T_{NPA}, it was treated at the higher level, while all of the remaining orbitals were considered to be low-level. This selection is denoted as R1. In another set of calculations, we included not only the metal but also the atoms directly involved in the bond breaking/formation taking place. These correspond to the oxygen and the sulfur to which it covalently binds. This selection is denoted as R2. In the SO case, we opted to include the full substrate in the high-level region, since it would be arbitrary to select a single oxygen in some of the steps. In a final selection, denoted as R3, we added to R2 the atoms coordinated to molybdenum. The number of orbitals in the high-level region for each selection/system is given in the caption of Figure 3, as well as the total number of valence orbitals for comparison. As one can observe, one starts

dx.doi.org/10.1021/ct5008313 | J. Chem. Theory Comput. XXXX, XXX, XXX−XXX

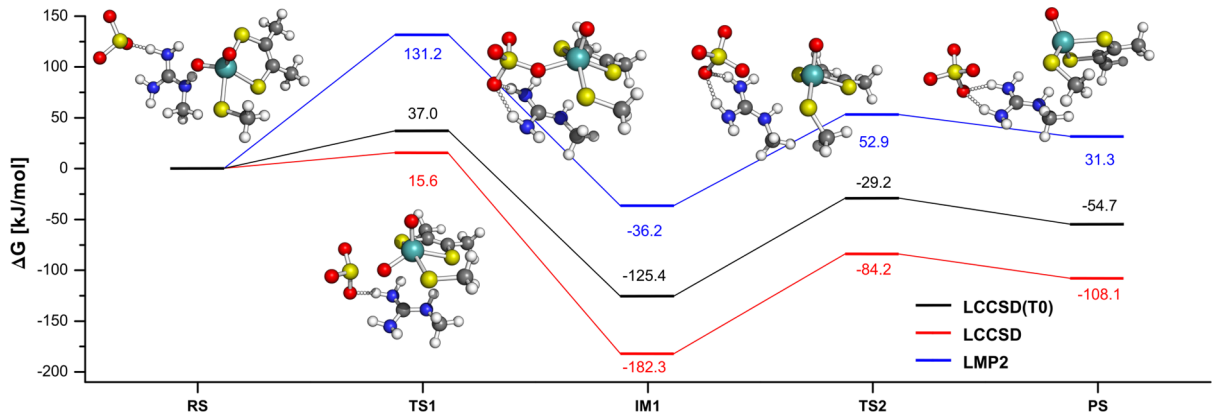

Figure 4. Free energies (in kJ/mol) along the reaction path of SO. Corrections to the electronic energies were taken from ref 23.

by including about one-third of the orbitals in the high-level region in R1, and this increases to roughly one-half of the orbitals in the case of R3.

3. COMPUTATIONAL DETAILS

All of the wave function calculations were carried out with the Dunning cc-pVTZ basis set[39] in combination with the aug-cc-pVTZ-PP orbital basis and the Stuttgart/Dresden ECP28MDF pseudopotential,[40] the latter used for the description of Mo. In all of the local correlation calculations, the orbitals were Pipek–Mezey-localized[41] and the domains determined according to the NPA criterion with T_{NPA} = 0.03*e*. For the calculation of reaction pathways, it is important to keep a consistent domain definition. Although in the SO case no particular attention was necessary, domain merging was needed in the DMSOR reaction.[42] This guaranteed that the number of orbitals in the high-level region was kept constant for all stationary points.

Density fitting (DF) approximations were used throughout,[29,43,44] so we will leave out the "DF" prefix for the remainder of the text. The Coulomb and exchange fitting basis sets used were def2-TZVPP for Mo and cc-pVTZ/JKFIT for all other atoms.[45,46] In all of the correlation calculations, use was made of cc-pVTZ/MP2FIT (with the def2-TZVPP fitting basis for Mo).[47,48] The pair-approximation criteria were changed from the default, strong pairs being defined as within a distance of 3 bohr and close pairs as within 5 bohr. This is in accordance with our previous study of DMSOR.[22] Strong orbital pairs were fully included in the coupled cluster treatment, while the close pairs were treated at the MP2 level but partly included in the triples calculation.[49]

All of the structures used in our calculations were taken from previous investigations of the reaction mechanisms. In the case of DMSOR, the geometries from ref 22 were used, and structures for the SO mechanism were retrieved from ref 23. The DMSOR active site was modeled with two 1,2-dimethyldithiolate (DMDT) ligands, replacing the molybdopterin. A methoxide was used in place of a serine residue. The SO active site was modeled with a DMDT ligand, methyl thiolate (replacing a cysteine residue), and a methylguanidinium interacting with the substrate, which was used instead of an arginine and contributes to the charge neutrality of the cluster. In the original study, molybdopterin was modeled with ene-1,2-dithiolate, so two methyls were added to change the ligand to DMDT. This way, the molybdopterin ligands were modeled by the same group in all of the calculations. For results given as free energies, all of the corrections to the electronic energies were taken from the same sources. In the case of SO, we used the values of Hernandez-Marin and Ziegler[23] and added as a correction the difference between our wave function result and the energy computed with the BP86 functional using the same basis sets. These are taken to be close to the DFT energies from the original study, where the same functional was applied in combination with triple-ζ-quality STO basis sets.

All of the calculations were carried out with a development version of Molpro 2012.1.[50,51]

4. RESULTS AND DISCUSSION

4.1. SO Reaction. The reaction mechanism for the sulfite oxidation in the SO system includes a first step wherein the sulfur atom of SO_3^{2-} binds to the equatorial oxygen of the Mo complex. The O atom transfer then proceeds through two transition states. In TS2 the O atom transfer is completed with full dissociation of the bond to Mo. As previously mentioned, an arginine residue was included in our model and was found to be in close interaction with the substrate. However, it is not directly involved in the reaction. In Figure 4 we have plotted the LMP2, LCCSD, and LCCSD(T0) results for the aforementioned steps in order to obtain a clear comparison of the different methods. The structures of the stationary points are also depicted.

The LCCSD(T0) free energies show that TS1 lies higher in energy than TS2. This is in agreement with previous studies on the same mechanism, including our CC results using a different model.[23,26] Even though the highest barrier is found in the transition from IM1 to the final products, one should take into account that when proceeding from TS1 to TS2, the transition is dominated by a mode running along the S–O–Mo bonds. Given also the similarity of the three structures, it should not be expected that the energy will dissipate. The active site should have enough energy to overcome the second barrier after traversing TS1. Therefore, we take the bottleneck step to be TS1, with a barrier of 37 kJ/mol. On the basis of kinetic measurements, it is possible to deduce an experimental barrier of about 51 kJ/mol.[52] The difference of 14 kJ/mol is significant but to be expected given the simplicity of the model and the use of a continuum solvent description (which is included in the free energy corrections taken from ref 23). It has been noted how strongly the choice of the dielectric constant may influence this reaction barrier.[26] Also noteworthy is the fact that the product state (PS) is higher in energy than the optimized intermediate (IM1). This is due to missing solvent interactions in the outgoing SO_4^{2-} anion and Mo complex. In particular, the

dx.doi.org/10.1021/ct5008313 | J. Chem. Theory Comput. XXXX, XXX, XXX–XXX

latter should coordinate with water after the reaction is concluded, stabilizing the complex. We did not consider this final step in our calculations.

Upon comparison of the methods with the LCCSD(T0) values as reference, it is clear that LMP2 shows significant deviations. The latter consistently overestimates the relative energies by about 80−90 kJ/mol. The difference is somewhat smaller in the case of LCCSD, which goes in the opposite direction. One should expect a failure of LMP2 when the formal oxidation state of the metal is changed. It is then somewhat surprising that already for TS1, which is an early transition state, the results show such a strong deviation. In this structure, the Mo−O bond is still kept. One would expect that a divergence, if it were to happen, would occur starting from the IM1 structure, where the Mo−O bond has been significantly changed. This should at some point correspond to the transition from the formal Mo^{VI} oxidation state to Mo^{IV}. This reasoning seems to hold in the case of LCCSD. The difference in the TS1 relative energy is only 21.4 kJ/mol. In comparison, the LMP2 error is as large as 94.2 kJ/mol.

It is evident that LMP2 fails in the description of this system. We computed the T1 diagnostic along the reaction path and found values ranging between 0.020 and 0.027, depending on the structure chosen. These values already indicate some multireference character (>0.02) but are still below previously suggested thresholds for the application of CCSD(T) (0.04[53] or even 0.05[54]). They do not change significantly from structure to structure. We furthermore checked the RHF/UHF stability of the reference wave function, which was revealed to be no issue in any stationary point.

We next were interested in replicating the high-level LCCSD(T0) results with the use of smaller orbital spaces where the LCCSD(T0) method was applied while the remaining system was treated at the LMP2 level. As detailed in Methods, three region selections were tested, consisting of the Mo atom (R1), the atoms directly involved in the reaction (R2), and a last set of results where all atoms directly coordinated to Mo were also included (R3). The results are listed in Table 1. It can be seen that the main effects are already

Table 1. Relative Electronic Energies (in kJ/mol) Computed for the SO Reaction at Different Levels of Theory

		LCCSD(T0):LMP2			
structure	LMP2	R1	R2	R3	LCCSD(T0)
RS	0.0	0.0	0.0	0.0	0.0
TS1	90.1	−16.7	−6.2	−5.2	−4.1
IM1	−68.3	−160.1	−158.2	−156.4	−156.9
TS2	65.7	−21.7	−19.2	−16.9	−16.5
PS	55.6	−33.4	−31.5	−29.3	−30.4

captured with the smallest selection possible (R1). Simply correlating the orbital space in the direct vicinity of the Mo atom is sufficient to correct most of the deficiencies in the LMP2 model. This falls in line with what one would expect, as the main problem in the LMP2 description should be linked to the metal orbital pairs. However, some deviations relative to the highest level were still found. In the case of TS1, the error is still above 10 kJ/mol. Otherwise, the differences between LCCSD(T0):LMP2 and LCCSD(T0) are quite constant. It should be noted that such a small region size would not be feasible in a subtractive QM/QM calculation (e.g., ONIOM). Building a model out of a single atom to compute corrections would be impossible since the electronic state in the model and the full system should be the same. This would require replicating the electronic configuration from the complex. Even if a few more atoms are added (selections R2 and R3), the situation would not be much different.

The results for the remaining selections are within the expected ranges. The R2 values show errors of about 2−3 kJ/mol. Given the type of approximations usually required in computational studies of enzymatic active sites, this would already be a reasonable compromise. The results were finally found to converge with R3, with only the TS1 error lying above 1 kJ/mol.

Finally, we wanted to take a closer look into multireference effects in our system. In particular, the truncation of the virtual space could influence the values of the diagnostics, since the number of accessible configurations is significantly reduced. With this objective in mind, we built smaller model systems mimicking the reactant $[Mo^{VI}(O)_2(SH)_3]^-$ and product $[Mo^{IV}(O)(SH)_3]^-$ states. These are shown in Figure 5. The structures were optimized at the B3LYP/def2-TZVP level of theory, including the respective effective core potential on Mo.

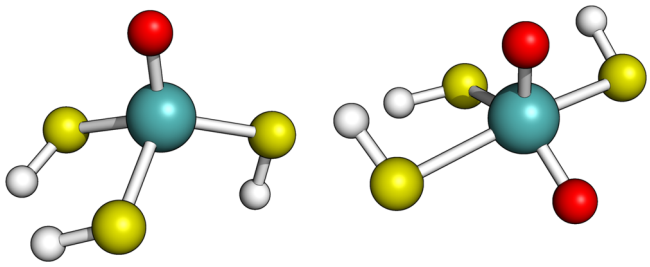

Figure 5. Model systems: (left) $[Mo^{IV}(O)(SH)_3]^-$ and (right) $[Mo^{VI}(O)_2(SH)_3]^-$.

Full canonical CCSD(T) and LCCSD(T0) calculations were carried out for comparison. In both systems we obtained values of the T1 diagnostic smaller than 0.04 independent of the method used. In the $[Mo^{IV}(O)(SH)_3]^-$ complex, the T1 diagnostic values from the CCSD(T) and LCCSD(T0) calculations were 0.033 and 0.028, respectively. In the case of $[Mo^{VI}(O)_2(SH)_3]^-$, we obtained 0.026 and 0.025. In both complexes, the double amplitudes did not exceed the value of 0.05, which is taken as the threshold to identify strong multireference character.[54] These values show that the diagnostics give similar results for local and canonical calculations even though the single excitations are restricted to orbital domains.

4.2. DMSOR Reaction. We now turn to the results obtained in the DMSOR system. In this case, the O binds to the Mo center and is abstracted, breaking the bond to the sulfur atom in DMSO/DMS. Also, in contrast to the SO active site, in DMSOR the Mo is bound to two molybdopterin ligands. In our calculations, these were again substituted with DMDT.

Comparing the general reaction profiles given in Figure 6, one can again observe a strong deviation between LMP2 and LCCSD(T0), but only for TS2 and the products. The error is particularly significant (>100 kJ/mol) when calculating the total reaction energy. On the other hand, the LCCSD results are in closer agreement, lying within 20 kJ/mol of the reference. The T1 diagnostics in this pathway are close to the values obtained in the SO case, again hinting at weak multireference character. It should also be noted that the pattern in the differences is

dx.doi.org/10.1021/ct5008313 | J. Chem. Theory Comput. XXXX, XXX, XXX−XXX

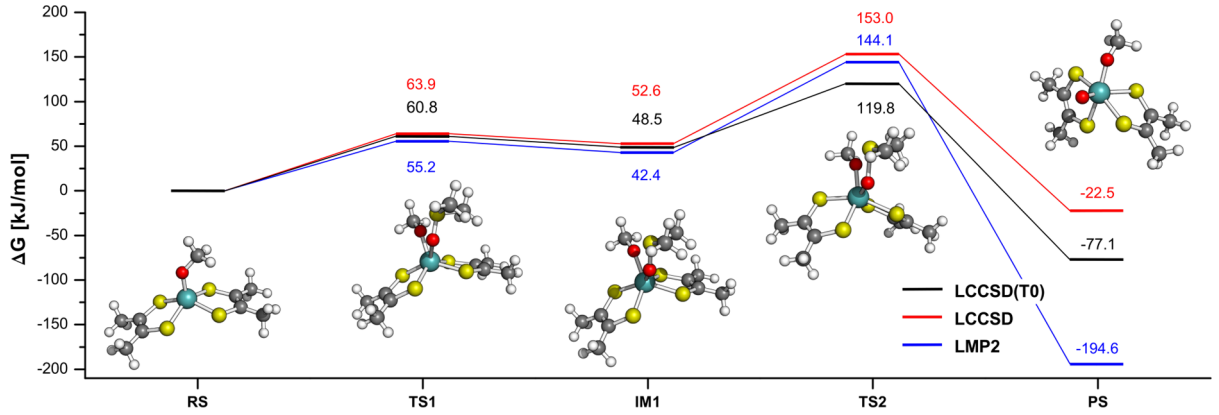

Figure 6. Free energies (in kJ/mol) along the reaction path of DMSOR. Corrections to the electronic energies were taken from ref 22.

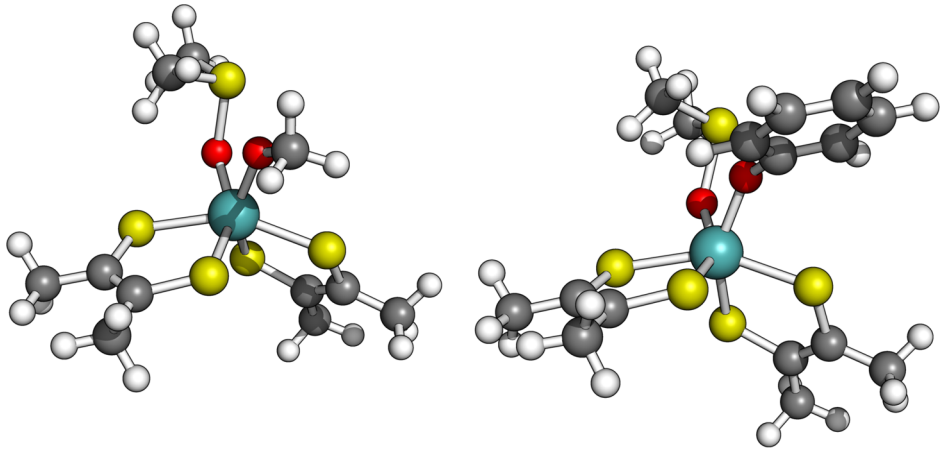

Figure 7. TS2 structures for (left) the DMSOR cluster model and (right) a biomimetic complex of the same enzyme.

quite close to DMSOR. The reactions proceed in opposite directions, so the reference structure corresponds to Mo^{VI} in one case and Mo^{IV} in the other.

In our previous mechanistic study of this system,[22] a biomimetic model was also considered.[55] The chemical formula of the latter ($[Mo(DMDT)_2(PhO)]^-$) is close to that of the cluster used to represent the DMSOR active site, differing only in one of the ligands (PhO^- instead of CH_3O^-). The mechanisms followed are the same, and we were able to identify similar stationary points. Figure 7 shows the TS2 geometries for the two complexes. Since the two sets of structures were available, we decided to also include the $[Mo(DMDT)_2(PhO)]^-$ complex in our tests. The results are given in Table 2.

Comparing the values between the CH_3O^- and PhO^- ligands, one observes that the LCCSD(T0) results are quite close for each stationary point. The LMP2 values, on the other hand, exhibit much larger errors when the phenoxide is included. This effect should be connected to the aromatic character of the ligand. Curiously enough, even the smallest LMOMO calculation already corrects for this behavior.

Examining the individual LMOMO values, one observes somewhat smaller differences than in the SO reaction for the R1 region. The same cannot be said about the R2 and R3 selections. In the case of the CH_3O^- ligand, the LCCSD-(T0):LMP2 (R3) deviations are within 1 kJ/mol except for the product state. The latter case shows a deviation of about 3 kJ/mol. In the case of the PhO^- ligand, the deviations are somewhat larger but still below 5 kJ/mol for all of the structures.

Table 2. Relative Electronic Energies (in kJ/mol) Computed for the DMSOR Reaction at Different Levels of Theory, including the Biomimetic Complex (PhO)

		LCCSD(T0):LMP2			
structure	LMP2	R1	R2	R3	LCCSD(T0)
		CH_3O			
RS	0.0	0.0	0.0	0.0	0.0
TS1	15.5	17.7	19.1	21.4	21.2
IM1	10.5	12.0	14.1	17.0	16.6
TS2	93.6	71.3	69.5	69.1	69.4
PS	−252.2	−140.9	−139.1	−138.0	−134.8
		PhO			
RS	0.0	0.0	0.0	0.0	0.0
TS1	28.8	26.4	26.5	25.6	23.1
IM1	8.2	6.7	9.4	12.1	12.0
TS2	87.4	58.4	56.5	55.5	57.1
PS	−257.4	−143.0	−141.2	−139.3	−134.9

In order to obtain a clearer picture of the efficiency of LMOMO in the two main reaction pathways, in Figure 8 we have plotted once again the free energies obtained at the LCCSD(T0) and LMP2 levels together with the LCCSD-(T0):LMP2 values for the smallest selection (R1). Although the latter are not sufficient to obtain converged values on each barrier height, there is a visible improvement. A qualitatively

dx.doi.org/10.1021/ct5008313 | J. Chem. Theory Comput. XXXX, XXX, XXX−XXX

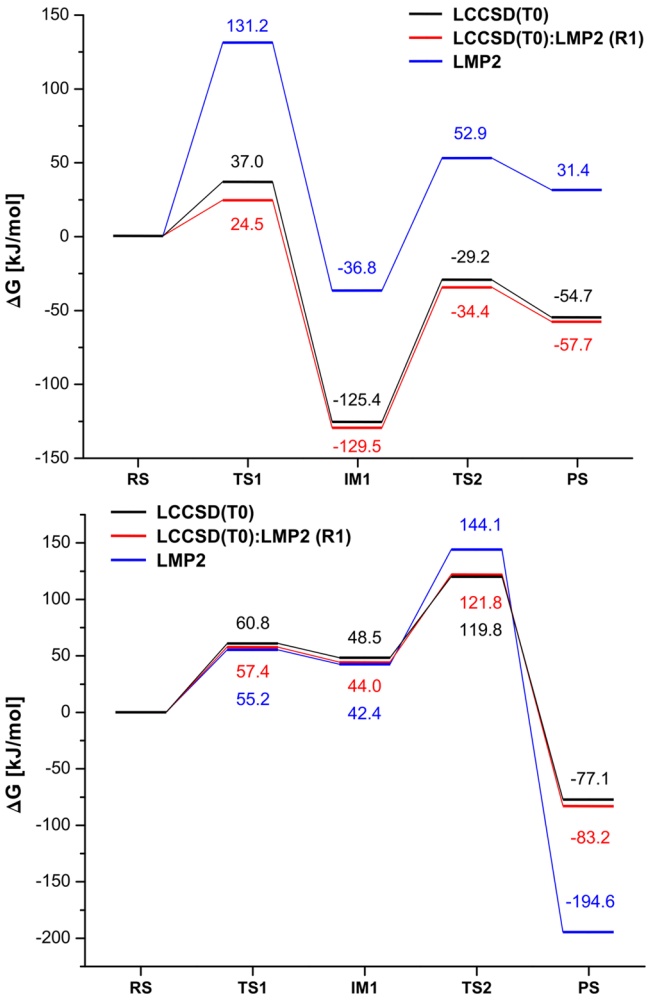

Figure 8. Free energy (in kJ/mol) reaction profiles for (top) SO and (bottom) DMSOR. The LMOMO results are shown for selection R1 in both cases.

correct picture is obtained for the overall profiles. As a last note, it should be mentioned that divergences between LCCSD(T0) and LMP2 similar to those observed here for SO and DMSOR have also been found in reactivity studies of aldehyde oxidoreductase, another Mo enzyme.[56]

5. CONCLUSIONS

We have explored the use of the LMOMO QM/QM hybrid scheme for the description of reaction pathways in catalytic metal complexes. The latter is formulated from the PAO-based family of local correlation methods, separating a molecular system into different regions according to the location of the orbital spaces. This allows one to specify arbitrarily small regions, in this case as small as a single atom, to be described at higher levels of theory within the MP2/CC hierarchy. We have applied the method to the reaction pathways of two related reactions involving Mo active centers. In both cases we have found that MP2 calculations are inadequate to describe the energetics of the system. There is no evidence for strong multireference character. However, on the basis of the T1 diagnostics and double-amplitude vectors, the inclusion of at least single excitations seems to be necessary.

The LMOMO LCCSD(T0):LMP2 calculations are in general able to replicate the reference LCCSD(T0) values. A large portion of the correction is already obtained by including only the metal center. However, adding the direct coordination shell to the latter is needed to converge the relative energies to within 1 kcal/mol for the majority of the stationary points. In general, our results seem to confirm that this is a promising approach for the calculation of reaction barriers in bioinorganic complexes. One alternative application of LMOMO LCCSD(T0):LMP2 calculations could also be as a first test of the stability/reliability of (L)MP2 calculations. On the basis of Figure 8, it seems to be sufficient to treat the metal atom at the CC level to roughly estimate the error. Furthermore, we have confirmed that the T1 diagnostics for full canonical, local, and hybrid LMOMO calculations fall in agreement. These are all valuable pieces of information that can be obtained at a relatively low cost.

■ ASSOCIATED CONTENT

Supporting Information

Energy corrections used to obtain the free energy paths together with the structures of the stationary points for both mechanisms. This material is available free of charge via the Internet at http://pubs.acs.org.

■ AUTHOR INFORMATION

Corresponding Author

*E-mail: rmata@gwdg.de. Phone: +49-(0)551-393149. Fax: +49-(0)551-3922202.

Funding

Financial support from the German Excellence Initiative through the Free Floater Research Group Program of the University of Göttingen is gratefully acknowledged. M.A. was supported through a Ph.D. scholarship from the International Research Training Group 1422.

Notes

The authors declare no competing financial interest.

■ REFERENCES

(1) Blomberg, M. R. A.; Borowski, T.; Himo, F.; Liao, R.-Z.; Siegbahn, P. E. M. *Chem. Rev.* **2014**, *114*, 3601−3658.
(2) Gutten, O.; Beššeová, I.; Rulíšek, L. *J. Phys. Chem. A* **2011**, *115*, 11394−11402.
(3) Dapprich, S.; Komáromi, I.; Byun, K. S.; Morokuma, K.; Frisch, M. J. *J. Mol. Struct.: THEOCHEM* **1999**, *461*, 1−21.
(4) Mata, R. A.; Werner, H.-J.; Schütz, M. *J. Chem. Phys.* **2008**, *128*, No. 144106.
(5) Pulay, P. *Chem. Phys. Lett.* **1983**, *100*, 151−154.
(6) Saebø, S.; Pulay, P. *Chem. Phys. Lett.* **1985**, *113*, 13−18.
(7) Krisiloff, D. B.; Carter, E. A. *Phys. Chem. Chem. Phys.* **2012**, *14*, 7710−7717.
(8) Riplinger, C.; Neese, F. *J. Chem. Phys.* **2013**, *138*, No. 034106.
(9) Li, W.; Piecuch, P. *J. Phys. Chem. A* **2010**, *114*, 6721−6727.
(10) Rolik, Z.; Kállay, M. *J. Chem. Phys.* **2011**, *135*, No. 104111.
(11) Basu, P.; Stolz, J. F.; Smith, M. T. *Curr. Sci.* **2003**, *84*, 1412−1418.
(12) Webster, C. E.; Hall, M. B. *J. Am. Chem. Soc.* **2001**, *123*, 5820−5821.
(13) Thapper, A.; Deeth, R. J.; Nordlander, R. *Inorg. Chem.* **2002**, *41*, 6695−6702.
(14) Mohr, M.; McNamara, J. P.; Wang, H.; Rajeev, S. A.; Ge, J.; Morgado, C. A.; Hillier, I. H. *Faraday Discuss.* **2003**, *124*, 413−428.
(15) McNamara, J. P.; Hillier, I. H.; Bhachu, T. S.; Garner, C. D. *Dalton Trans.* **2005**, 6695.
(16) McNamara, J. P.; Joule, J. A.; Hillier, I. H.; Garner, C. D. *Chem. Commun.* **2005**, *2*, 177−179.
(17) Hofmann, M. *J. Mol. Struct.: THEOCHEM* **2006**, *773*, 59−70.

(18) Hofmann, M. *Inorg. Chem.* **2008**, *47*, 5546−5548.
(19) Hernandez-Marin, E.; Ziegler, T. *Can. J. Chem.* **2010**, *88*, 683−693.
(20) Tenderholt, A. L.; Wang, J. J.; Szilagyi, R. K.; Holm, R. H.; Solomon, E. I. *J. Am. Chem. Soc.* **2010**, *132*, 8359−8371.
(21) Tenderholt, A. L.; Hodgson, K. O.; Hedman, B.; Holm, R. H.; Solomon, E. I. *Inorg. Chem.* **2012**, *51*, 3436−3442.
(22) Li, J.-L.; Mata, R. A.; Ryde, U. *J. Chem. Theory Comput.* **2013**, *9*, 1799−1807.
(23) Hernandez-Marin, E.; Ziegler, T. *Inorg. Chem.* **2009**, *48*, 1323−1333.
(24) Thapper, A.; Deeth, R. J.; Nordlander, E. *Inorg. Chem.* **1999**, *38*, 1015−1018.
(25) Pal, K.; Chaudury, P. K.; Sarkar, S. *Chem.—Asian J.* **2007**, *2*, 956−964.
(26) van Severen, M.-C.; Andrejić, M.; Mata, R. A.; Nordlander, E.; Ryde, U. *J. Biol. Inorg. Chem.* **2014**, *19*, 1165−1179.
(27) Garrett, R. M.; Johnson, J. L.; Graf, T. N.; Feigenbaum, A.; Rajagopalan, K. V. *Proc. Natl. Acad. Sci. U.S.A.* **1998**, *95*, 6394−6398.
(28) Hampel, C.; Werner, H.-J. *J. Chem. Phys.* **1996**, *104*, 6286−6297.
(29) Werner, H.-J.; Manby, F. R.; Knowles, P. *J. Chem. Phys.* **2003**, *118*, 8149−8160.
(30) Werner, H.-J.; Schütz, M. *J. Chem. Phys.* **2011**, *135*, No. 144116.
(31) Boughton, J. W.; Pulay, P. *J. Comput. Chem.* **1993**, *14*, 736−740.
(32) Reed, A. E.; Weinstock, R. B.; Weinhold, F. *J. Chem. Phys.* **1985**, *83*, 735−746.
(33) Mata, R. A.; Werner, H.-J. *Mol. Phys.* **2007**, *105*, 2753−2761.
(34) Kaminsky, J.; Mata, R. A.; Werner, H.-J.; Jensen, F. *Mol. Phys.* **2008**, *106*, 1899−1906.
(35) Sen, S. S.; Hey, J.; Herbst-Irmer, R.; Eckhardt, M.; Mata, R. A.; Roesky, H. W.; Scheer, M.; Stalke, D. *Angew. Chem., Int. Ed.* **2011**, *50*, 12510−12513.
(36) Dieterich, J. M.; Oliveira, J. C. A.; Mata, R. A. *J. Chem. Theory Comput.* **2012**, *8*, 3053−3060.
(37) Michel, R.; Nack, T.; Neufeld, R.; Dieterich, J. M.; Mata, R. A.; Stalke, D. *Angew. Chem., Int. Ed.* **2013**, *52*, 734−738.
(38) Andrejić, M.; Mata, R. A. *Phys. Chem. Chem. Phys.* **2013**, *15*, 18115−18122.
(39) Dunning, T. H., Jr. *J. Chem. Phys.* **1989**, *90*, 1007−1023.
(40) Peterson, K. A.; Figgen, D.; Dolg, M.; Stoll, H. *J. Chem. Phys.* **2007**, *126*, No. 124101.
(41) Pipek, J.; Mezey, P. G. *J. Chem. Phys.* **1989**, *90*, 4916−4926.
(42) Mata, R. A.; Werner, H.-J. *J. Chem. Phys.* **2006**, *125*, No. 184110.
(43) Schütz, M.; Werner, H.-J.; Lindh, R.; Manby, F. R. *J. Chem. Phys.* **2004**, *121*, 737−750.
(44) Polly, R.; Werner, H.-J.; Manby, F. R.; Knowles, P. J. *Mol. Phys.* **2004**, *102*, 2311−2321.
(45) Weigend, F. *J. Comput. Chem.* **2008**, *29*, 167−175.
(46) Weigend, F. *Phys. Chem. Chem. Phys.* **2002**, *4*, 4285−4291.
(47) Hellweg, A.; Hättig, C.; Hofener, S.; Klopper, W. *Theor. Chem. Acc.* **2007**, *117*, 587−597.
(48) Weigend, F.; Köhn, A.; Hättig, C. *J. Chem. Phys.* **2002**, *116*, 3175−3183.
(49) Mata, R. A.; Werner, H.-J.; Thiel, S.; Thiel, W. *J. Chem. Phys.* **2008**, *128*, No. 025104.
(50) Werner, H.-J.; Knowles, P. J.; Knizia, G.; Manby, F. R.; Schütz, M.; Celani, P.; Korona, T.; Lindh, R.; Mitrushenkov, A.; Rauhut, G.; Shamasundar, K. R.; Adler, T. B.; Amos, R. D.; Bernhardsson, A.; Berning, A.; Cooper, D. L.; Deegan, M. J. O.; Dobbyn, A. J.; Eckert, F.; Goll, E.; Hampel, C.; Hesselmann, A.; Hetzer, G.; Hrenar, T.; Jansen, G.; Köppl, C.; Liu, Y.; Lloyd, A. W.; Mata, R. A.; May, A. J.; McNicholas, S. J.; Meyer, W.; Mura, M. E.; Nicklass, A.; O'Neill, D. P.; Palmieri, P.; Peng, D.; Pflüger, K.; Pitzer, R.; Reiher, M.; Shiozaki, T.; Stoll, H.; Stone, A. J.; Tarroni, R.; Thorsteinsson, T.; Wang, M. *MOLPRO: A Package of Ab Initio Programs*, version 2012.1; http://www.molpro.net.
(51) Werner, H.-J.; Knowles, P. J.; Knizia, G.; Manby, F. R.; Schütz, M. *Wiley Interdiscip. Rev.: Comput. Mol. Sci.* **2012**, *2*, 242−253.
(52) Wilson, H. L.; Rajagopalan, K. V. *J. Biol. Chem.* **2004**, *279*, 15105−15113.
(53) Martin, J. M. L.; Taylor, P. R. *J. Phys. Chem.* **1996**, *100*, 6047−6056.
(54) Jiang, W.; DeYonker, N. J.; Wilson, A. K. *J. Chem. Theory Comput.* **2012**, *8*, 460−468.
(55) Lim, B. S.; Sung, K. M.; Holm, R. H. *J. Am. Chem. Soc.* **2000**, *122*, 7410−7411.
(56) Dieterich, J. M.; Werner, H.-J.; Mata, R. A.; Metz, S.; Thiel, W. *J. Chem. Phys.* **2010**, *132*, No. 035101.